

An environment for the analysis and reconstruction of archaeological objects

C. Laugerotte and N. Warzée

Systèmes Logiques et Numériques, Université Libre de Bruxelles, Belgium

Abstract

To assist archaeologists in their work of analysis and reconstruction of archaeological objects from their fragments, several environments have been developed in which virtual fragments can be manipulated. As a part of these environments, an important tool consists in automating the search for correct assemblages between two 3D objects by evaluating their matching surfaces. In this paper, we describe a new environment for computer aided reconstruction of archaeological objects and we propose a new method to estimate the quality of an association based on a surface area evaluation.

1. Introduction

In recent years, number of computerised tools have appeared to assist archaeologists in their work of analysis and reconstruction of archaeological objects. These tools are justified for several reasons. Firstly, manual handling of fragments may be long and tedious because of their great number and/or their large size. Moreover, fragments may be fragile or subject to deterioration when handled. By exploiting virtual representations of fragments, their manipulation and study may be made easier. At last, much additional information (essentially metric information) can be obtained and used to propose virtual reconstructions.

We develop an environment in which virtual fragments can be manipulated. This environment is inspired by the computer aided tools cited in the "related work" section and by the methodology used by the archaeologists themselves. It contains different automatic and semi-automatic computerised tools to analyze fragments and get accurate geometric information which is difficult to access in a manual way. As a concrete case, our aim is to provide tools to assemble and analyze an architecture from the fragments exhumed under the floor of Saints-Michel-et-Gudule main collegiate church in Brussels (Belgium) [BF98].

Among these tools, an important one is the quality evaluation of an association between two fragments. In this paper, we use a technique exploiting information provided by the graphic cards [PKT02] and we propose a new method to evaluate the assemblage quality. It is based on the areas

of the surfaces implied in the assemblage and takes into account the specificities of our environment.

The paper is organized as follows. Related work concerning the computerised tools applied to archaeology is treated in section 2. In section 3, we present the methodology we follow, we describe the environment we developed and how an association is performed. In section 4, we consider the evaluation of an assemblage. Results are given and discussed in section 5. Finally, conclusion and future work are considered in section 6.

2. Related Work

The first computerised graphic tools proposed the visualization and the manipulation of virtual representations of fragments saved in a database [KRC*97, Lev00]. Next, analysis methods were introduced to automate the features extraction and the fragmented objects reconstruction. Taking into account the type of fragments and their complexity, different approaches were developed.

Two-dimensional objects were the first ones to be treated. Indeed, in the literature related to computer vision and 2D object recognition, several techniques can be applied to planar fragments such as contour extraction and silhouettes matching [Wol90, dGLS02]. Another approach, based on the exploitation of geometric features, has been developed by the Forma Urbis Romae Project [fur] where incised lines appearing on marbles slabs are identified manually and annotated according to characteristics such as position, angle and

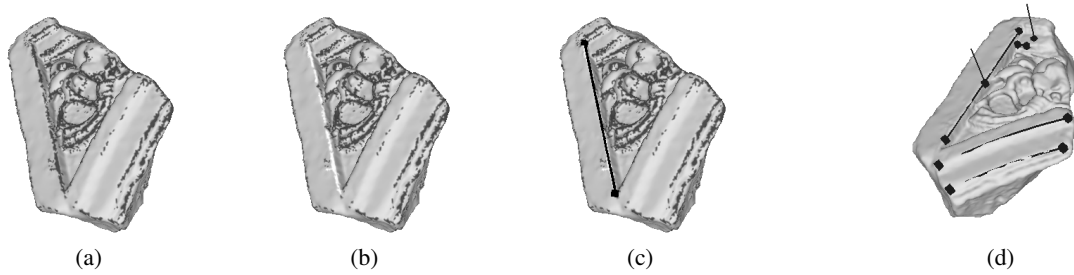


Figure 1: Extraction of a line: (a) automatic extraction of significant vertices (b) manual selection of relevant vertices (c) approximation of the selected vertices with a line and (d) visualization of the same fragment after the extraction of 2 arcs or circle, 2 lines and 2 planes.

type. Next, associations are done according to these characteristics.

The study of 3D objects was initially introduced for fragments of ancient potteries on which break curves are extracted and assimilated to 3D curves [KK01]. A signature is then defined for this 3D curve with its arc length, its curvature and its torsion [KW87]. An algorithm for the matching of two 3D curves is proposed in [UT99]. The use of splines is also treated in [KWH90].

In a parallel direction to the assemblage of pottery fragments, other characteristics can be extracted and used for the classification. In the *Computer Aided Classification of Ceramics* project [SK02a, SK02b], a documentation system for fragments was developed, based on the features extraction (axis of rotation, profile), the fragments classification and ceramics reconstruction. In a similar way, the *STITCH project* [LCJ*01] proposed other approaches [CM02, WC04].

In the general case of arbitrary fragments, few tools exist. Some previous work generalized the problem of finding similar regions in two surfaces [RB89, BS97]. More recently, a method using information computed by graphic cards is exploited to evaluate the assemblage of fragments of various origins (statue, architecture, ...) [PKT02] and has been extended by combining it with former methods [PK03]. This method consists in moving objects until a function, named *matching error* associated to the assemblage quality and based exclusively on geometric data, reaches a minimum. Our method uses the technique exploited in this latter method and we propose a new evaluation to estimate the assemblage quality.

3. Methodology

The methodology used by the archaeologists [Ath02] consists in grouping fragments by similar features appearing on them (color, geometry, deterioration, nature of the material, ...). Then, associations between individual fragments in a set are attempted by matching the extracted features.

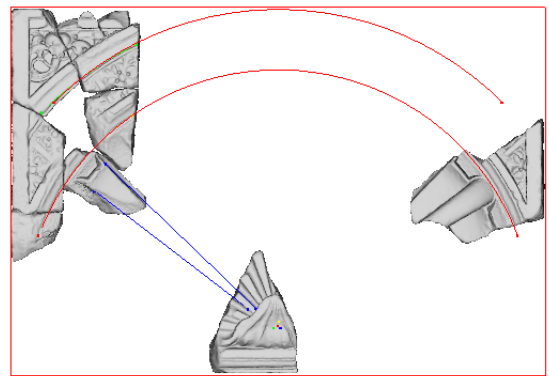


Figure 2: Virtual reconstruction of a niche with extrapolation of the geometric primitives used to associate the fragments.

In this paper, we extend an approach based on this methodology and already introduced in [LADW03] to propose a complete environment. It uses exclusively geometric features deduced from meshes generated by a scanning system and can be decomposed into four main steps: 3D acquisition of the fragments, characterization of the meshes, associations between fragments and evaluation of the assemblage quality. These different steps are detailed in the following sections.

3.1. 3D Acquisition

To expect relevant results, highly-accurate 3D models of the stone fragments were demanded since the level of detail on the fragments can be less than one millimeter. This, and the fragility of the fragments, suggested a non-contact acquisition technique. For this purpose, a system based on the laser stripe triangulation was chosen and the device we used is the 3D scanner FastScan™ commercialized by Polhemus [Pol]. Afterwards, the different fragments are scanned, resulting in dense triangular meshes.

3.2. Characterization of the fragments

A few methods exist to extract features from 3D meshes (for example planes) but they do not allow to treat lines and arcs of circle. For this reason, the fragments characterization is made in a semi automatic way, assisted by a set of existing 3D tools, in order to consider directly relevant features and to focus on the feasibility of the general methodology.

Until now, the features we treat are simple geometric primitives such as points, lines, arcs of circle and planes appearing on the fragments. Concerning lines and arcs of circle, vertices of potential interest, defined as belonging to ridges or valleys, are identified automatically by thresholding their principal curvatures [Car76] computed directly from the mesh [Tau95, MDSB02, CSM03]. Additional selection tools and conditions on the vertices can be considered [RKS00, WB01]. Then, from these preselections, a manual selection is performed to isolate significant vertices from which a geometric primitive is deduced by a least squares method [Ebe00]. Concerning planes, they are identified from surfaces generated by a naive but efficient segmentation process [PKT02]. To illustrate these different steps, Fig 1 shows the extraction of a line and a fragment with its extracted features.

3.3. Associations

Once these geometric features are extracted and approximated by geometric primitives, they are regarded as connections to find associations between the corresponding fragments. The associations are attempted automatically by orienting and translating the objects in order to respect a continuity between similar geometric primitives. In practice, two lines are oriented to be parallel and translated to merge their extremities. Two arcs of circle are associated by orienting the fragments in order to place the arcs of circle in the same plane. Then, the tangents at their extremities are made parallel and the extremities are merged. Concerning the planes, they are oriented in the same direction and merged.

Moreover, the merging of the extremities leads to situations where an overlap may occur. To avoid this situation, one of the fragments is translated in the direction of the association (*i.e.* along a line or an arc of circle) until there is no more overlap. This configuration is then associated to a contact between the two objects.

3.4. Constraints

During the assemblage process, 3D objects are submitted to a system of constraints and dependencies in order to reduce the degrees of freedom. Constraints restrict the motion of an object according to the orientation or position of a geometric primitive. Dependencies occur when an association is validated between two objects. Then, moving one object leads to move the other with which it is associated and a constraint

applied to one object is also applied to the other. This system of constraints and dependencies is automatically managed when an association is validated. Nevertheless, the user can interact and precise some constraints manually (orienting a line, fixing a point, ...).

The interest of this approach is that it allows the association of disjointed fragments. Moreover, the extrapolation of geometric primitives allows to analyze the architecture from the fragments. These two situations are illustrated in Fig. 2 presenting the virtual reconstruction of a Renaissance niche realized by selecting manually associations between fragments through geometric primitives. At first, disjointed fragments were assembled by imposing a translation constraint along two sets of two lines appearing on the basis of the niche and on a fragment on the upper left part. Moreover, an estimation of the symmetry was deduced with several characteristics appearing on the fragments (centers of the two arcs of circle, center of the arcs leaving the basis of the niche) and an estimation of the dimensions of the niche ($1m \times 0.7m$) was confirmed by adding a new fragment on the right side and by extrapolating the arcs of circles.

4. Evaluation of an Association

From now, we treat adjacent fragments assemblage and we propose a method to determine if an association is relevant enough to be submitted to the archaeologists for validation.

4.1. Properties of the Evaluator

First of all, we need a method to evaluate the relevance of an assemblage in an independent way, *i.e.* without any comparison with another assemblage. Indeed, in our environment, constraints between fragments restrict the set of possible associations and the evaluations are reduced to only a few potential associations. Therefore, we aim to provide a normalized evaluation. Moreover, during the 3D acquisition process, noise appears according to the accuracy of the scanning system (with our system, tests composed of several series of 100 scans of the same surface revealed that the variance of the 3D points distribution is between 0.07 and 0.2 mm^2 according to the geometric complexity of the fragment and the number of sweeps applied). To manage this situation, the evaluator should be robust against noise. Another important fact is that the fragments are often damaged by erosion, leading to reduce perfect matching situations between adjacent fragments. Therefore, a pure differential approach is not appropriate and a more tolerant evaluation is needed. At last, the assemblage quality should be reduced when the surfaces implied are small in order to privilege assemblages implying large surfaces.

4.2. Distance Map

The approach we adopt is based on the approximation of the surfaces implied in the association (S_i) and the ones corre-

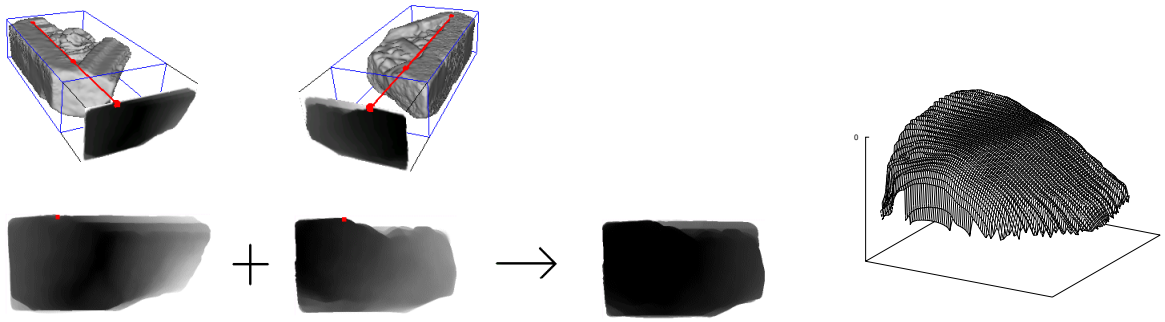


Figure 3: Evaluation of the distance between two fragments: extraction of the distance maps for the two fragments by projecting them onto a plane and evaluation of the distance $d(u, v)$ after merging the geometric primitives implied in the association. The surface on the right is a 3D representation of the distance $d(u, v)$. The area near 0 indicates a low distance between the fragments and the distance increases when the surface falls.

sponding to a good matching (S_m). These surfaces are determined by computing the distances separating the two fragments. For this, a plane P is placed in front of each object perpendicularly to the direction of the association. Then, for all the points (u, v) on P , the distance between P and the object in the direction perpendicular to P is computed and stored in a distance map $d(u, v)$. When no point of the fragment is in front of a point (u, v) , the distance is undefined.

The information contained in the distance map can be obtained in an attractive and a quick way from graphic cards as it has been proposed in [PKT02]. Indeed, to render a 3D scene in orthographic projection mode, graphic cards calculate the distances between a plane and the objects in the scene (in our case, the scene is reduced to one object). This information, stored in the *z-buffer*, provides directly the needed distance maps.

Let $d_1(u, v)$ and $d_2(u, v)$ be the two distance maps associated to the two fragments. The distance between the two fragments is deduced from these two distance maps, by flipping horizontally one of the distance map (let's say $d_2(u, v)$ becoming $d'_2(u, v)$) and by merging the projected points implied in the association in order to make the points facing each other (as illustrated in Fig. 3).

The points set where $d_1(u, v)$ and $d'_2(u, v)$ are simultaneously defined is called the surface of intersection S_i

$$S_i = \{(u, v) | d_1(u, v) \neq \infty, d'_2(u, v) \neq \infty\}$$

The evaluation of the association is computed on this set (a 2D slice is represented in Fig. 4).

Moreover, the minimal distance d_{min} separating the two fragments is defined as follows

$$d_{min} = \min \left\{ (d_1(u, v) + d'_2(u, v)) | (u, v) \in S_i \right\}$$

and it is used to determine the distance between the two frag-

ments on each point (u, v) by the following relation

$$d(u, v) = d_1(u, v) + d'_2(u, v) - d_{min}$$

4.3. Evaluators

From the information stored in the distance maps, methods are proposed to evaluate the association. A first method consists in integrating this distance over S_i [PKT02]. Another method proposes to compute a *matching error* by averaging the variations of the slopes between the two surfaces, S_{1_i} and S_{2_i} , implied in the matching [PKT02]. Nevertheless, these two evaluations are not normalized and they are noise sensitive. In the first case, noise may affect the minimal distance d_{min} . In the second case, noisy surfaces may produce important variations of slopes which are accumulated over S_i .

We propose a new method to evaluate the assemblage quality by thresholding the function $d(u, v)$ to define the matching surface as follows

$$S_m = S_i \cap \{(u, v) \in \mathcal{R}^2 | d(u, v) \leq t_1\}$$

where t_1 is a positive parameter.

It is important to notice that all the entire intersection surface is not implied in an association: some parts of the surfaces may be far apart and a missing fragment might exist between them. Therefore, a new thresholding is applied to reduce the surface of intersection in which the association will be evaluated, giving the new surface

$$S'_i = \{(u, v) \in \mathcal{R}^2 | d(u, v) \leq t_2\}$$

where t_2 is a new positive parameter such that $t_1 \leq t_2$.

Finally, the assemblage quality is evaluated by the coefficient γ

$$\gamma(t_1, t_2, \alpha, n) = \left(1 - \frac{A'_i - A_m}{A'_i + A_m}\right) G$$

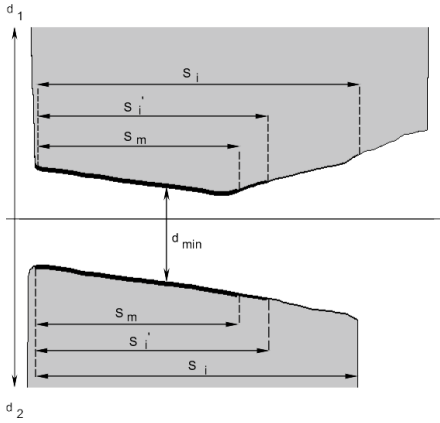


Figure 4: Partition of the surfaces implied in the evaluation of a matching: Surfaces of intersection S_i , reduced surfaces of intersection S_i' and surfaces of matching S_m .

where A_m and A_i' are respectively the areas of the surfaces S_m and S_i' , and G is a gain function reducing the importance of associations attempted on small surfaces. For this latter, we use an expression inspired by the Butterforth filter

$$G(\alpha, n) = \frac{1}{1 + \left(\frac{\alpha}{A_m}\right)^{2n}}$$

where α is a cutoff area and n is the order of the gain function. Therefore, a satisfying matching will produce a value γ close to 1 while a value close to 0 will indicate an irrelevant association (in the following, we express γ as a percentage).

Concerning the evaluation of A_i' and A_m , the sum of the pixels can be used and corresponds to the projected area of S_m onto the plane perpendicular to the direction of the association. But, in some configurations, the area of the projected matching surface is quite inferior to the real area of the matching surface (an example of such configuration is given in Fig. 5). Therefore, an approximation for the real areas would give better results.

4.4. Real Areas Approximation

Let $S(x(u, v), y(u, v), z(u, v))$ be a parametric surface. The area of this surface is determined by its first fundamental form [Car76] as follows

$$A_S = \iint_S \left\| \frac{\partial \vec{S}(u, v)}{\partial u} \times \frac{\partial \vec{S}(u, v)}{\partial v} \right\| dudv$$

In our case, the real areas of the surfaces are determined by exploiting the functions $d_1(u, v)$ and $d_2(u, v)$. Then, we set

$$\vec{S}(u, v) = \begin{cases} S_x(u, v) = u \\ S_y(u, v) = v \\ S_z(u, v) = d(u, v) \end{cases}$$

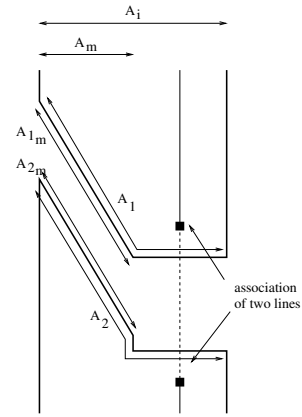


Figure 5: Configuration where the projected surface of matching A_i does not represent correctly the quality of the association.

and we obtain the following expression for the area of a surface S

$$A_S = \iint_S \left\| \begin{pmatrix} 1 \\ 0 \\ \frac{\partial d(u, v)}{\partial u} \end{pmatrix} \times \begin{pmatrix} 0 \\ 1 \\ \frac{\partial d(u, v)}{\partial v} \end{pmatrix} \right\| dudv$$

which leads to the following expression

$$A_S = \iint_S \sqrt{1 + \left(\frac{\partial d(u, v)}{\partial u}\right)^2 + \left(\frac{\partial d(u, v)}{\partial v}\right)^2} dudv$$

A numerical version of the distances $d_1(u, v)$ and $d_2(u, v)$ is provided by the distance map as explained above. By using the finite differences to evaluate the partial derivatives $\frac{\partial d(u, v)}{\partial u}$ and $\frac{\partial d(u, v)}{\partial v}$, we obtain the following discretised version

$$\tilde{A}_S = \sum_{(i, j) \in S_i} \sqrt{1 + \Delta d_u(i, j)^2 + \Delta d_v(i, j)^2}$$

where

$$\begin{aligned} \Delta d_u(i, j) &= d(i + 1, j) - d(i, j) \\ \Delta d_v(i, j) &= d(i, j + 1) - d(i, j) \end{aligned}$$

when $d(i + 1, j)$, $d(i, j + 1)$ and $d(i, j)$ are defined.

This new formulation leads us to consider different areas. The intersection area A_{1i} (resp. A_{2i}) corresponding to the surface associated to the first (resp. second) object is deduced from $d_1(u, v)$ (resp. $d_2(u, v)$) where $d(u, v)$ is defined and less than a threshold t_2 . Moreover, the matching area $A_{1,m}$ (resp. $A_{2,m}$) corresponding to the first (resp. second) object is deduced from $d_1(u, v)$ (resp. $d_2(u, v)$) where $d(u, v)$ is less than a threshold t_1 .

5. Results and Discussion

These different techniques for evaluating the quality of an assemblage are tested with synthetic data in order to val-

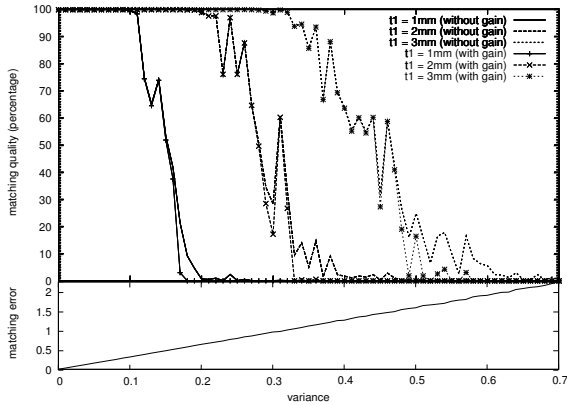


Figure 6: Robustness against noise is tested with different values for the first threshold. On the upper figure, the three first curves represent $1 - \frac{A_i - A_m}{A_i + A_m}$ while the three last ones represent $\gamma(t_1, t_2, \alpha, n)$ where the gain function effect appears when the surfaces areas decrease (the values of the parameters are $\alpha = 60\text{cm}^2$ and $n = 3$). On the lower figure, the curve represents the matching error under the same perturbations and shows its linear evolution from which it is delicate to define what is a correct assemblage.

idate their behaviors in specific configurations. They are subsequently tested with real data. For all the tests, the z -buffer resolution is fixed in such a way the distance between two adjacent pixels (by considering a 4-neighborhood) represents 1mm . This choice is motivated by the fact that the meshes generated by our 3D acquisition system are defined with a decimation close to 1mm . Moreover, the parameters α , n , t_1 and t_2 have been chosen according to the data (synthetic or real) and precised experimentally. We present results and discuss them in the following sections. The time needed to compare two surfaces depends on the size of the z -buffers. During our tests, the resolution generally encountered was between 60×60 and 120×120 pixels and the time for one comparison was between 0.5 and 0.8sec.

5.1. Synthetic Data

To validate our approach against noise, we take two planar surfaces matching perfectly and representing two $20 \times 10\text{cm}$ plaques. Then, we evaluate the quality of the matching after the application of a noise defined by a normal distribution with increasing variances. The results we obtain are gathered in Fig. 6 and show that our evaluation is robust against noise (regarding the characteristics of our scanning system) when the threshold is at least superior to 2mm , after what the relevance of the assemblage decreases quickly.

Concerning the gain function, it is tested and validated by considering the same two planar surfaces facing each other, and by applying a rotation on one of them around one of

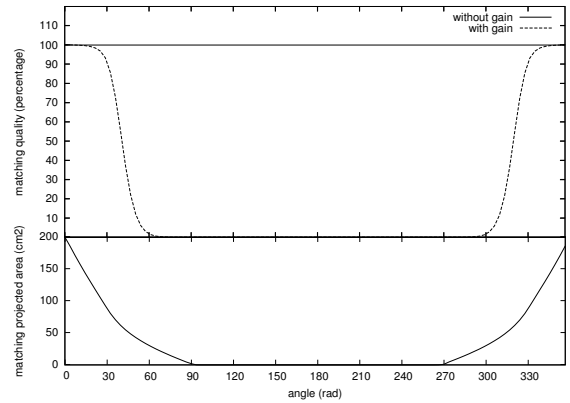


Figure 7: The relevance of the association (upper figure) decreases according to the surface area implied in the matching (lower figure). In the upper figure, the first curve, constant, represents $1 - \frac{A_i - A_m}{A_i + A_m}$, while the other represents $\gamma(t_1, t_2, \alpha, n)$ with $\alpha = 60\text{cm}^2$ and $n = 3$.

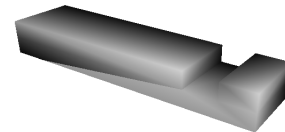


Figure 8: Synthetic data used to illustrate and validate the properties of the evaluator.

its corner. The results are shown in Fig. 7 and illustrate the interest of the gain function which minimizes the association quality when surface area implied in the association decreases.

After these tests validating the properties expected for the evaluator, we attempt associations between the synthetic 3D models showed in Fig. 8. The geometric primitives used to assemble them are the edges of the objects and we treat four associations. The results are gathered in Fig. 9. As expected, the first association, presenting a complete matching, provides the best result. The second and third associations illustrate different behaviours depending on the matching area involved in the assemblage. In particular, for the third assemblage, both real areas implied in the assemblage produce a high assemblage quality while the projected area is not relevant and produces an inappropriate assemblage quality measure. The fourth assemblage illustrates the case of small matching surfaces and their restricted importance.

5.2. Real Data

Tests have been made on the eight fragments belonging to the upper left part of the Renaissance niche reproduced in

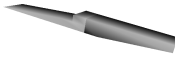
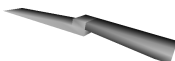


Associations	Projected areas			Real areas					
	A_i (cm^2)	A_m (cm^2)	γ	A_{1_i} (cm^2)	A_{2_i} (cm^2)	A_{1_m} (cm^2)	A_{2_m} (cm^2)	γ_1	γ_2
	200	200	100%	200	200	200	200	100%	100%
	122	100	86.07%	119.4	325.74	95.52	95.52	83.74%	42.73%
	200	100	63.39%	1702.01	1105.61	959.92	959.92	72.12%	92.95%
	24	2	0%	220	21.89	0	0	0%	0%

Figure 9: Results of tests on synthetic data. The left part contains the values for A_i , A_m and γ by considering projected areas. The right part considers real areas and γ for each object. The interest of real areas appears clearly in the third assemblage where all the effective matching surface is taken into account. All the γ values are computed with $\alpha = 60cm^2$ and $n = 3$.

Fig. 2. As a first step, a set of different features (composed of 2 points, 33 lines, 8 arcs of circle and 6 planes) has been extracted manually. Based on these primitives, a set of 206 associations were possible (by considering all the associations between two lines and between two arcs of circle) and tested automatically to select the most relevant ones. In the case of lines association, a plane has been identified on each fragment, inducing a constraint.

5.2.1. Association Validation

To illustrate the different situations we met, we only consider the fragments reproduced in Fig. 3 and some evaluations of the different possible assemblages are gathered in Fig. 10.

It appears that the *matching error* is irrelevant on the entire surface of intersection since the lowest value is not associated to the correct assemblage. Nevertheless, the evaluation on the thresholded intersection surface S_i^t makes sense and reveals the correct assemblage.

Concerning the evaluations based on the surface areas, similar results are observed and small surfaces are easily dismissed. Regarding the results obtained with all the set of fragments, it appears that assemblages presenting a value γ superior to 55% can be treated such as potential assemblages. This low threshold is mainly due to the accuracy of the 3D models generated by the scanning system and the erosion undergone by the fragments, altering their perfect matching.

To compare the efficiency of the two matching evaluations, their ROC curve are gathered in Fig. 11 and show that our assemblage quality evaluation is more strict than the *matching error*.

At last, as these two evaluators do not consider the same

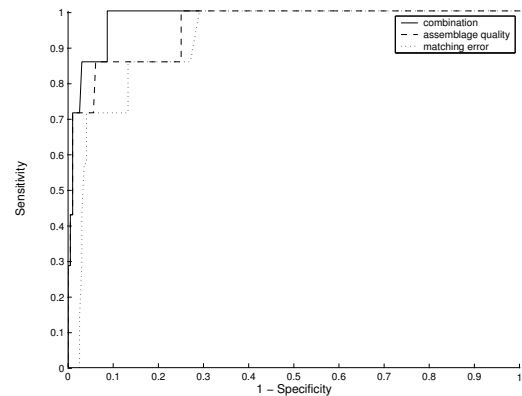


Figure 11: ROC curve comparing the two matching evaluations.

approach, they are complementary and better results are obtained from their combination. Therefore, a set of potential associations selected by the highest values γ is confirmed by a *matching error* inferior to a threshold experimentally deduced from noise appearing in the 3D models. To produce the combination curve in Fig. 11, the threshold we used is 0.8.

5.2.2. Comparison of Associations

In the previous section, strong constraints are set and only one configuration is possible between the fragments. Nevertheless, if we treat associations only through lines, rotations are still allowed around this line, resulting several potential assemblages. Therefore, a comparative approach is applied

by evaluating a discretized version of the set of possible rotations.

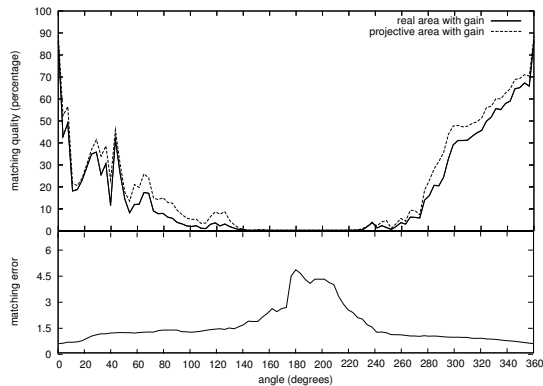


Figure 12: Area-based evaluations

The results obtained with the evaluation of the real areas of the surfaces implied in the assemblages are shown in Fig 12. As an initial position, the two objects are correctly associated. Next, a rotation is indicated in degrees on the x-axis and the corresponding assemblage quality is indicated on the y-axis by a percentage representing γ . These results are compared with the *matching error* evaluated on the same thresholded intersection surfaces.

In a general way, we notice that γ expresses correctly the assemblage quality. Firstly, the best assemblage is detected by the highest value γ without any ambiguity. Secondly, when small surfaces are implied by the association, γ takes into account this situation and we notice the interest of the gain function with lower values for γ .

These results are compared with those obtained by evaluating the *matching error*. As expected, it is low near the right association as well and the best association is identified by the lowest value.

6. Conclusion and future work

An environment, based on the methodology used by the archaeologists themselves, has been presented to assist analysis and study of archaeological objects. It consists in identifying geometric features appearing on the fragments and in using them to propose assemblages by respecting a continuity between them. The first results have shown the interest of this approach since it is not limited to adjacent fragments and provide further results concerning a small architecture dimensions. On the other hand, features should appear on the fragments and they should be identified on the mesh to find connections between them.

In the case of adjacent fragments, an evaluation of the quality of an assemblage has been proposed in order to

identify automatically the relevant associations. This evaluation has been validated on synthetic data and on a set of eight fragments (only results from two of them are reproduced here in Fig. 10). Moreover, they have been compared to already existing methods and the results show that, even though the validation by an archaeologist is essential, it is possible to efficiently select relevant assemblages, potentially saving the archaeologist considerable time sorting through hundreds or thousands of fragments.

Future work might expand within this environment to include the addition of new geometric primitives and more complex rules of associations between the fragments. Other useful improvements include the automatic extraction of features and their approximation.

Acknowledgements

This work is granted by the "Région de Bruxelles-Capitale".

The authors would like to thank Philippe Van Ham, Denis Haumont, Xavier Baele and Olivier Debeir for discussions and ideas which made this paper possible.

The archaeological fragments we worked with were excavated at the Brussels Saints-Michel-et-Gudule collegiate church by Prof. Bonenfant. The authors would like to thank him to allow us to work with this material.

References

- [Ath02] ATHANASIOS V.: *Virtual Conservation: the reconstruction of a fragmented object with the aid of three-dimensional computer models*. PhD thesis, Royal College of Art, 2002.
- [BF98] BONENFANT P., FOURNY M.: Chronique des fouilles de la société - fouilles archéologiques à la cathédrale de bruxelles. *Annales de la Société Royale d'archéologie de Bruxelles* 62 (1998), 225–257.
- [BS97] BAREQUET G., SHARIR M.: Partial surface and volume matching in three dimensions. *IEEE Transactions on Pattern Analysis and Machine Intelligence* 19 (1997).
- [Car76] CARMO M. D.: *Differential geometry of curves and surfaces*. Prentice Hall, 1976.
- [CM02] CAO Y., MUMFORD D.: Geometric structure estimation of axially symmetric pots from small fragments. In *Signal Processing, Pattern Recognition, and Applications (SPPRA)* (june 2002).
- [CSM03] COHEN-STEINER D., MORVAN J.-M.: Restricted delaunay triangulations and normal cycle. In *Proceedings of the nineteenth annual symposium on Computational geometry* (2003), ACM Press, pp. 312–321.

- [dGLS02] DA GAMA LEITÃO H. C., STOLFI J.: A multiscale method for the reassembly of two-dimensional fragmented objects. *IEEE Transactions on Pattern Analysis and Machine Intelligence* 24, 9 (2002), 1239–1251.
- [Ebe00] EBERLY D. H.: *3D Game Engine Design*. Morgan Kaufmann Publishers, september 2000.
- [fur] Digital forma urbis romae project website : <http://graphics.stanford.edu/projects/forma-urbis/>.
- [KK01] KONG W., KIMIA B. B.: On solving 2d and 3d puzzles using curve matching. In *IEEE Conference on Computer Vision and Pattern Recognition (CVPR)* (2001).
- [KRC*97] KALVIN A. D., REMY A., CASTILLO L. J., MORLA K., NOLASCO E., PRADO J., FERNANDEZ V., FRANCO R., WIESE G.: Computer-aided reconstruction of a pre-inca temple ceiling in peru. In *Computer Applications in Archaeology (CAA 97)* (apr 1997).
- [KW87] KISHON E., WOLFSON H.: 3-d curve matching. In *Proceeding of the AAAI Workshop on Spatial Reasoning and Multi-sensor Fusion* (1987), pp. 250–261.
- [KWH90] KISHON E., WOLFSON H., HASTIE T.: 3-d curve matching using splines. In *Proceedings of the first european conference on Computer vision* (1990), Springer-Verlag New York, Inc., pp. 589–591.
- [LADW03] LAUGEROTTE C., ANAGNOSTOPOULOS P., DIERKENS A., WARZÉE N.: Towards a virtual 3d reconstruction of a rood-screen from its archaeological fragments. In *Enter the Past - Computer Applications in Archaeology (CAA 2003)* (2003).
- [LCJ*01] LEYMARIE F. F., COOPER D. B., JOUKOWSKY M. S., KIMIA B. B., LAIDLAW D. H., MUMFORD D., VOTE E. L.: The shape lab - new technology and software for archaeologists. In *"Computing Archaeology for Understanding the Past"* (CAA 2000) (2001), Archaeopress Oxford U., (Ed.), pp. 79–89.
- [Lev00] LEVOY M.: Digitizing the forma urbis romae. In *presented at the Siggraph "Digital Campfire" on Computers and Archeology Snowbird, Utah* (apr 2000), pp. 359–362.
- [MDSB02] MEYER M., DESBRUN M., SCHRÖDER P., BARR A. H.: Discrete differential-geometry operators for triangulated 2-manifolds. In *International Workshop on Visualization and Mathematics 2002 (Vismath 2002)* (May 2002), pp. 426–433.
- [PK03] PAPAIOANNOU G., KARABASSI E. A.: On the automatic assemblage of arbitrary broken solid artefacts. *Image & Vision Computing* 21, 5 (2003), 401–412.
- [PKT02] PAPAIOANNOU G., KARABASSI E., THEOHARIS T.: Reconstruction of three-dimensional objects through matching of their parts. *IEEE Transactions on Pattern Analysis and Machine Intelligence* 24, 1 (January 2002), 114–124.
- [Pol] POLHEMUS: <http://www.polhemus.com/>.
- [RB89] RADACK G., BADLER N. I.: Local matching of surfaces using boundary-centered radial decomposition. *Computer Vision, Graphics, and Image Processing* 45, 3 (1989), 380–396.
- [RKS00] ROESSL C., KOBBELT L., SEIDEL H.-P.: Extraction of feature lines on triangulated surfaces using morphological operators. In *Smart Graphics 2000, AAAI Spring Symposium* (2000), pp. 71–75.
- [SK02a] SABLATNIG R., KAMPEL M.: Computer aided classification of ceramics. In *Virtual Archaeology - Proceedings of the VAST2000 Euroconference* (2002), Niccolucci F., (Ed.), Arezzo, Oxford, Archaeopress, pp. 77–82.
- [SK02b] SABLATNIG R., KAMPEL M.: Model-based registration of front- and backviews of rotationally symmetric objects. *Computer Vision and Image Understanding* 87, 1 (2002), 90–103.
- [Tau95] TAUBIN G.: Estimating the tensor of curvature of a surface from a polyhedral approximation. In *Fifth International Conference on Computer Vision (ICCV'95)* (1995).
- [UT99] UCOLUK G., TOROSLU I.: Automatic reconstruction of broken 3-d surface objects. *Computers and Graphics* 23, 4 (August 1999), 573–582.
- [WB01] WATANABE K., BELYAEV A.: Detection of salient curvature features on polygonal surfaces. *Computer Graphics Forum* 20, 3 (2001), 385–392.
- [WC04] WILLIS A. R., COOPER D. B.: Bayesian assembly of 3d axially symmetric shapes from fragments. In *Conference on Computer Vision and Pattern Recognition (CVPR'04)* (2004), pp. 82–89.
- [Wol90] WOLFSON H. J.: On curve matching. *IEEE Trans. Pattern Anal. Mach. Intell.* 12, 5 (1990), 483–489.

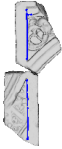



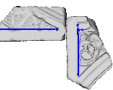
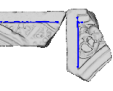

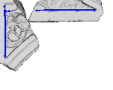
Associations	Matching error		Real areas					
	without thresh- olding	with thresh- olding	A_{1_i} (cm^2)	A_{2_i} (cm^2)	A_{1_m} (cm^2)	A_{2_m} (cm^2)	γ_1	γ_2
	7.42	1.00	7.66	6.71	2.02	1.82	41.52%	42.14%
	6.96	0.53	28.59	29.10	21.71	22.02	86.32%	86.14%
	5.59	0.61	11.43	12.17	0.81	0.93	4.61%	7.92%
	5.68	0.91	6.69	6.63	2.54	2.55	54.99%	55.40%
	2.99	0.73	8.85	9.41	0.85	0.92	7.30%	9.53%
	3.79	0.90	5.78	6.25	1.86	1.86	48.12%	45.34%
	4.47	0.82	5.11	5.09	1.88	1.89	53.09%	53.63%
	4.97	0.97	2.59	2.78	0.64	0.64	4.74%	4.44%

Figure 10: Results of assemblages between two real fragments with $t_1 = 3mm$, $t_2 = 7mm$, $\alpha = 90mm^2$ and $n = 3$. The first column is an illustration of the attempted assemblages. The two next columns gather the matching error computed on the entire surface and on a surface thresholded by t_2 . The other columns gather the evaluations for the areas of intersection, the areas of matching and the value γ for each fragment.